Magneto-optical activity of f-f transitions and properties of $4f$ states in single-crystal $DyFe_3(BO_3)_4$

A. V. Malakhovskii,* A. L. Sukhachev, A. Yu. Strokova, and I. A. Gudim
L. V. Kirensky Institute of Physics, SB RAS, 660036, Krasnoyarsk, Russia
(Received 23 January 2013; revised manuscript received 24 June 2013; published 2 August 2013)

Magnetic circular dichroism and polarized optical absorption spectra of single-crystal $DyFe_3(BO_3)_4$ were measured in the region of the crystal transparency from 8700 to 16 000 cm^{-1} in the temperature range from 90 K up to room temperature. Spectra of *d-d* and *f-f* transitions were separated, and *f-f* transitions ${}^6H_{15/2} \rightarrow {}^6(F_{9/2} + H_{7/2})$, ${}^6F_{7/2}$, ${}^6F_{5/2}$, and ${}^6F_{3/2}$ were studied. From these measurements, temperature dependences of the paramagnetic magneto-optical activity (MOA) of the electric dipole-forbidden *f-f* transitions were obtained. It was revealed that, in contrast to allowed transitions, temperature dependences of the MOA of some *f-f* transitions substantially deviate from the Curie-Weiss law. The theories of MOA of allowed and *f-f* transitions were considered and the experimental results obtained were accounted for. Circular polarizations in magnetic field and linear polarizations of absorption lines were determined. The Zeeman splitting of some absorption lines were found. Symmetries of the crystal field states were analyzed on the bases of the obtained results in D_3 local symmetry approximation. A small splitting ($\approx$16.5 cm^{-1}) between the two lowest sublevels of the ground manifold was detected, and symmetries of these states were identified as $E_{1/2}$ ($M = \pm 13/2$) and $E_{3/2}$ ($M = \pm 15/2$), respectively. Deviation of the local symmetry of the Dy^{3+} ion from D_3 is small, and it was revealed that polarizations of the majority of absorption lines can be accounted for in the D_3 symmetry. This also testifies that in the process of some other electron transitions, the equilibrium configuration of the local environment deviates from D_3 symmetry stronger than it does in the ground state. In addition, it has been shown that the distortions depend not only on the excited but also on the initial state.

DOI: 10.1103/PhysRevB.88.075103 PACS number(s): 78.20.Ls, 78.40.Ha, 71.70.Ej

I. INTRODUCTION

Optical and magneto-optical properties of compounds containing $4f$ ions are widely studied because of the great importance of these compounds for optical applications. In particular, spectroscopic properties of dysprosium in different substances have been studied rather extensively. The majority of these works were devoted to optical absorption and luminescence,[1–8] with laser applications in mind. The spectroscopic and crystal field (CF) analysis of Dy^{3+} in $YAl_3(BO_3)_4$ (YAB) crystals, isostructural with the $DyFe_3(BO_3)_4$ crystal, was performed in Refs. 4, 6, and 7 based on absorption and luminescence measurements. Some rare earth (R) ferroborates of this structure refer to multiferroics, i.e., they simultaneously exhibit magnetic and electric order.[9–13] Magnetic circular dichroism (MCD) gives additional information about electronic states. In particular, it permits us to find the sign and value of the Zeeman splitting when it is not resolved directly. This, in turn, helps to identify initial and final states of the transition. MCD of the parity-forbidden *f-f* transitions gives definite information about the origin of intensity of the *f-f* transitions. All these advantages of MCD will be used in the present paper. The magneto-optical activity (MOA) of a number of R-containing glasses was first studied long ago.[14] It was found that the MOA practically does not depend on the glass matrix. However, the authors measured the Faraday effect in the region of transparency. This effect is due to allowed transitions in the ultraviolet spectral region. Van Vleck and Hebb[15] have shown that the paramagnetic MOA should be proportional to the paramagnetic susceptibility and, consequently, should follow the Curie-Weiss law. This statement was confirmed experimentally but also with the help of the Faraday effect connected with the allowed transitions. There are many works devoted to the MCD of the parity-forbidden *f-f* transitions in glasses[16–22] and in crystals[23–33] (to the best of our knowledge, only Ref. 30 deals with the Dy^{3+} ion). However, in the majority of these works, MCD was measured at one or several temperatures, and analysis of the results was devoted to the decomposition of the MCD on diamagnetic and paramagnetic parts but not to the properties and nature of the *f-f* transitions' MCD.

In the first part of the present investigation, absolute values and temperature dependences of the integral paramagnetic MOA of *f-f* transitions in a single-crystal $DyFe_3(BO_3)_4$ are measured, and the nature of the observations is analyzed and accounted for. In the second part, the fine structure of MCD and polarized absorption spectra are studied. Based on these results, symmetry properties of the $4f$ states are analyzed, and the influence of the electron transitions on the local environment of the optically excited $4f$ ions is discussed.

II. EXPERIMENTAL DETAILS

Single crystals of the $DyFe_3(BO_3)_4$ compound were grown, as described in Ref. 34. At room temperature, the crystal has trigonal symmetry with the space group $R32$ and the lattice constants $a = 9.534$ Å and $c = 7.560$ Å.[35] (Part of the structure is shown in Fig. 1.) The unit cell contains three formula units. Trivalent R ions occupy only one type positions with the D_3 symmetry. They are located at the center of trigonal prisms made up of six crystallography-equivalent oxygen ions. At $T \sim 280$ K, there is a structural phase transition,[36] presumably to the trigonal $P3_121$ phase, as it takes place in some

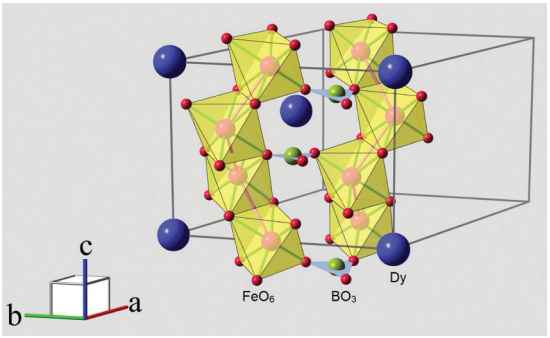

FIG. 1. (Color online) Part of the structure of the single-crystal $DyFe_3(BO_3)_4$.

other ferroborates.[37,38] Dy^{3+} ions are in C_2 positions in this structure. At 38 K, the single-crystal $DyFe_3(BO_3)_4$ undergoes a phase transition to an antiferromagnetically ordered easy-axis state.[34,36,39]

The polarized absorption and MCD spectra of $DyFe_3(BO_3)_4$ crystal were obtained in the temperature range from 90 K to room temperature. The absorption spectra were measured by the two beam technique using an automated spectrophotometer designed on the basis of the diffraction monochromator MDR-2. The MCD spectra were measured by the method of light-polarization modulation using a piezoelectric modulator (for details see Ref. 40). The spectral slit width at the absorption and MCD measurements was 0.4 nm (on average 5 cm^{-1} over the studied spectral region). The MCD was measured as the half difference of the circular dichroisms for plus and minus magnetic fields. Therefore, the possible in noncentro-symmetrical crystal natural circular dichroism was excluded. The absorption spectra measured in α polarization ($\vec{k} \parallel C_3$) and in σ polarization ($\vec{k} \perp C_3, \vec{E} \perp C_3$) coincide within the limit of experimental error and substantially differ from that measured in π polarization ($\vec{k} \perp C_3, \vec{E} \parallel C_3$), where C_3 is the triad axis of the crystal. This implies that the absorption mainly occurs through the electric dipole mechanism. The π and σ spectra were measured in the sample, cut in [110] plane (the thickness of the sample was 80 μm). Precise positions of polarization parallel to the main crystal axes were found according to the minimum transparency of the sample in crossed polarizers. MCD measurements were carried out at α polarization in a magnetic field of 5 kOe along the C_3 axis. The sample was put in a nitrogen gas flow cryostat. Accuracy of the temperature measuring was $\sim$1 K.

Complete absorption spectra of the $DyFe_3(BO_3)_4$ crystal in σ and π polarizations at room temperature are shown in Fig. 2 (decimal absorption coefficients). They consist of narrow lines corresponding to *f-f* transitions in Dy^{3+} ions and of wide bands due to *d-d* transitions in Fe^{3+} ions ($^6A_1 \rightarrow {}^4T_1$ and $^6A_1 \rightarrow {}^4T_2$ transitions in cubic CF notation). Until the strong absorption band edge at $E \sim 25\,000\ cm^{-1}$, there are no more *f-f* transitions. The *f-f* absorption spectrum should be separated from the total spectrum. On the first stage, the *f-f* absorption bands were erased from the total spectrum. The remaining spectrum, relating only to the *d-d* absorption, was approximated by the Gauss functions, and thus the *d-d* spectrum was obtained separately. Then this *d-d* spectrum was subtracted from the total spectrum, and the *f-f* spectrum was obtained separately.

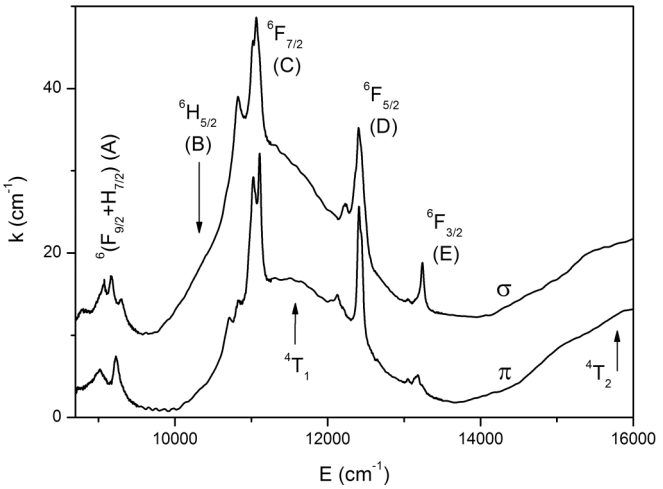

FIG. 2. Total polarized absorption spectra of the single-crystal $DyFe_3(BO_3)_4$ at room temperature.

III. PARAMAGNETIC MOA OF *f-f* TRANSITIONS

A. Properties of paramagnetic MOA of *f-f* transitions revealed in the experiment

MCD spectra of all studied *f-f* transitions are shown in Figs. 3–6. Contribution of the *d-d* transitions into the MCD is very small as compared with that of the *f-f* transitions and is not observed.

MCD conditioned by a pair of the Zeeman splitting components is described by the equation:

$$\Delta k = k_{m+}\phi(\omega,\omega_0 + \Delta\omega_0) - k_{m-}\phi(\omega,\omega_0 - \Delta\omega_0). \quad (1)$$

Here, k_+ and k_- are amplitudes of (+) and (−) circularly polarized lines; φ are form functions of (+) and (−) polarized lines. In majority of cases, the (−) polarized line has higher frequency ($\Delta\omega_0$ is negative). If the Zeeman splitting $\Delta\omega_0$ is much less than the line width, developing the form functions as series in $\Delta\omega_0$ one obtains

$$\Delta k = k_m c\varphi(\omega,\omega_0) + k_m \Delta\omega_0 \partial\varphi(\omega,\omega_0)/\partial\omega_0. \quad (2)$$

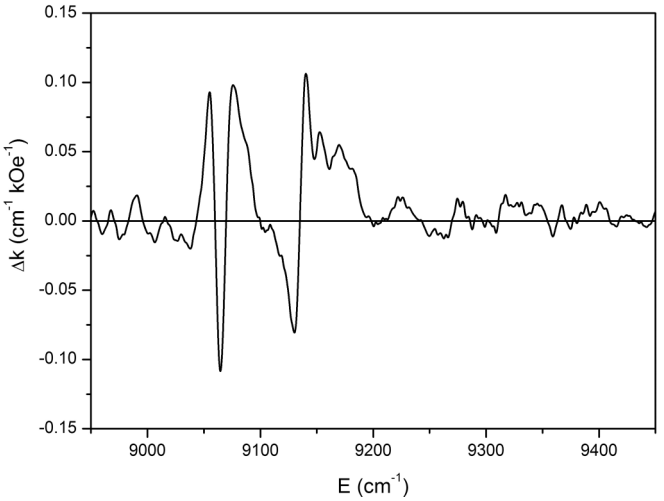

FIG. 3. MCD spectrum of the $^6H_{15/2} \rightarrow {}^6(F_{9/2} + H_{7/2})$ transition (*A* band) at 90 K.

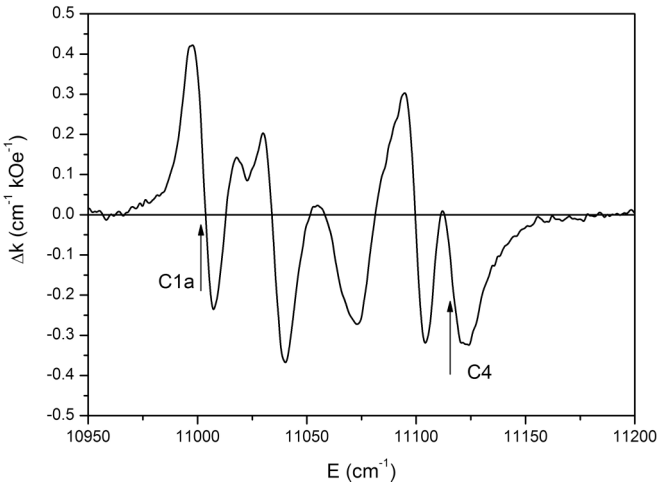

FIG. 4. MCD spectrum of the ${}^6H_{15/2} \rightarrow {}^6F_{7/2}$ transition (C band) at 90 K. Symbols $C1a$ and $C4$ correspond to the absorption lines identified in Sec. IV.

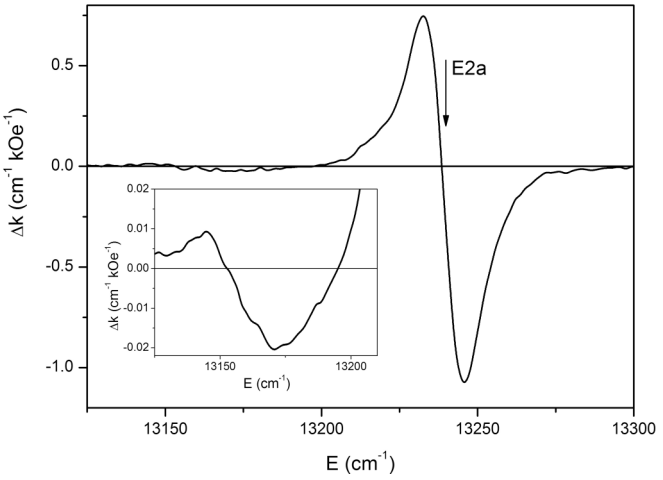

FIG. 6. MCD spectrum of the ${}^6H_{15/2} \rightarrow {}^6F_{3/2}$ transition (E band) at 90 K. Symbol $E2a$ corresponds to the absorption line identified in Sec. IV. Inset: fragment of the spectrum.

Here, $k_m = k_{m+} + k_{m-}$ is the amplitude of the line not split by the magnetic field and $c = (k_{m+} - k_{m-})/k_m$. The second term in (2) is the diamagnetic MCD, and the first one is the paramagnetic effect, whose dispersion coincides with that of absorption. Both for the one line and in the general case, when a complex absorption band consisting of a number of lines occurs, the integral paramagnetic MOA of the band is determined by the equation

$$c = \frac{\langle \Delta k(\omega) \rangle_0}{\langle k(\omega) \rangle_0} = C \frac{\mu_B H}{k_B (T - \theta)}. \quad (3)$$

Here, C is a dimensionless parameter of the MOA, k_B is the Boltzmann constant, and θ is the Curie-Weiss constant. In (3), it is supposed that the Curie-Weiss law is valid for the MOA according to Van Vleck and Hebb.[15] The fine structure of the MCD spectra (Figs. 3–6) is mainly due to diamagnetic effect, but from Eq. (2) it is evident that the diamagnetic effect gives zero as a result of integration over the absorption band (for the Gauss shape of the absorption line ω and ω_0 derivatives differ only in sign). MCD spectra of dysprosium-containing glasses[21,22] are structureless, and they approximately repeat the shape of the absorption spectra. Additionally, peak values of MCD in the glasses are about one order of magnitude smaller than those in the studied crystal. All these are the consequence of the space integration of MCD of the absorption centers with the random distribution of CFs and line positions in glasses. As a result, the average diamagnetic effect inside the band goes to zero and only the paramagnetic effect remains. A similar situation is observed in the electron-vibrational bands,[30] because a band of the quasilocal vibrations, but not the local monochromatic vibration, takes place there.

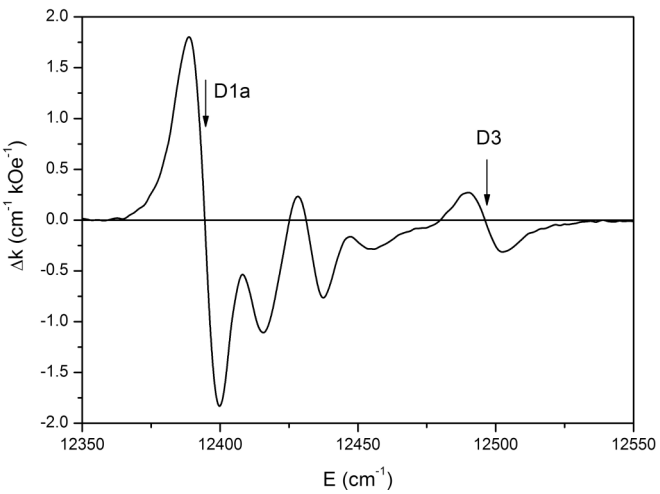

FIG. 5. MCD spectrum of the ${}^6H_{15/2} \rightarrow {}^6F_{5/2}$ transition (D band) at 90 K. Symbols $D1a$ and $D4$ correspond to the absorption lines identified in Sec. IV.

The zero moments of the MCD and absorption bands, the MOA of the transitions described by Eq. (3) and their temperature dependences were found from the experimental MCD and α-absorption spectra of the $DyFe_3(BO_3)_4$ crystal. If the MOA of the transition follows the Curie-Weiss law, then the dimensionless parameter C of the MOA in (3) should be independent of temperature. The $DyFe_3(BO_3)_4$ crystal has $\theta = -6.2$ K.[34] From the experimentally found temperature dependences of the MOA [c in Eq. (3)] and using the mentioned Weiss constant, temperature dependences of the parameter C for all absorption bands were obtained (Fig. 7). Some of them appeared to be substantially not constant, and the parameter C of the transition into the ${}^6(F_{9/2} + H_{7/2})$ state even changes sign at the temperature decrease (the same takes place in the glass Dy2 from Ref. 22). Parameters C at room temperature are shown in Table I. In the same table, the C parameters at room temperature are given for glasses from Ref. 22. They were obtained from the data of Ref. 22, according to Eq. (3), with the θ parameters found from magnetic measurements.[41]

The experimental results obtained pose several questions. (1) How can the sign and value of the f-f transitions MOA be explained? (2) Why are the MOA of the same f-f transitions different in different compounds? (For allowed transitions, they are approximately identical.) (3) Why do temperature dependences of the MOA of some f-f transitions not obey the Curie-Weiss law?

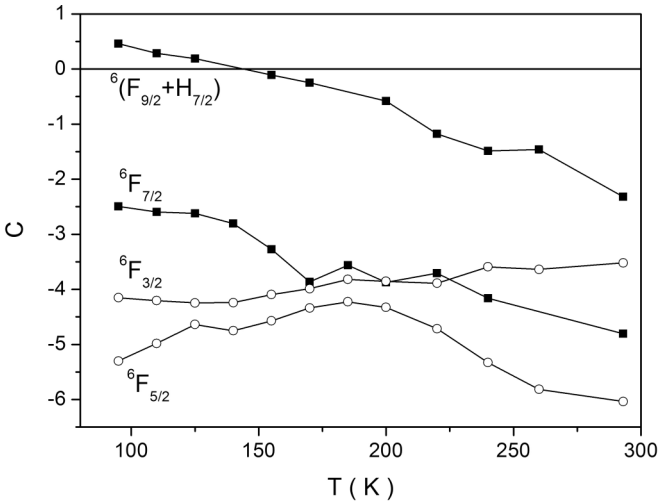

FIG. 7. Temperature dependences of integral paramagnetic MOA (C) of f-f transitions in the single-crystal $DyFe_3(BO_3)_4$.

B. Main properties of temperature-independent paramagnetic MOA and its contribution to the total paramagnetic magneto-optical effect

General theory of magneto-optical effects was presented in papers by Stephens[42,43] and in a series of subsequent works (e.g., Refs. 44 and 45). In addition to temperature-dependent paramagnetic magneto-optical effect (C term), Serber[46] and Stephens[42,43] introduced a temperature-independent paramagnetic effect (B term) or the "mixing effect," which can influence the temperature dependence of the total paramagnetic effect. The mixing effect can be rigorously obtained in the following way.[47,48] Consider an allowed electric-dipole transition between the multiplets I and F of an atom, which are split by different interactions (not with the magnetic field only) into states $i \in I$ and $f \in F$. The MCD [and magnetic circular birefringence (MCB)] per atom is known to be

$$\Delta\alpha_1 = (\alpha_1^+ - \alpha_1^-) = \frac{1}{\hbar}\sum_{i,f} f_i(T)\Delta p_{if}^{\pm}\varphi(\omega,\omega_{if},\gamma_{if}). \quad (4)$$

Here $\alpha_1^{\pm}$ is the polarizability of the atom for $\pm$ circularly polarized waves,

$$\Delta p_{if}^{\pm} = |\vec{d}_{if}^{+}|^2 - |\vec{d}_{if}^{-}|^2, \quad (5)$$

where $d_{if}^{\pm}$ are matrix elements of the electric-dipole moment of the transitions $i \to f$ for $(+)$ and $(-)$ circular polarizations, and

$$f_i(T) = \exp\left(-\frac{E_i}{kT}\right)\Big/\sum_i \exp\left(-\frac{E_i}{kT}\right) \quad (6)$$

is the thermal population of the i level of the ground multiplet. The functions φ are complex dispersion functions, where the real part describes the birefringence and the imaginary one describes the dichroism, ω_{if} and γ_i are frequency and width of the absorption line corresponding to the transition $i \to f$.

Let's write frequencies ω_{if} in the form: $\omega_{if} = \omega_0 + \Delta\omega_{if}$, where ω_0 is the frequency of the transition between the unsplit manifolds I and F, and $\Delta\omega_{if}$ is the shift of the frequency of the transition $i \to f$ relative to ω_0 as a result of splitting of the multiplets I and F by different interactions, including the magnetic field. If the frequency of observation is far from the resonance region, i.e., the MCB is observed, the dispersion functions are real. Their dependence on the line widths γ_{if} can be neglected; additionally, it can be written

$$\varphi'(\omega,\omega_{if}) \approx \varphi'(\omega,\omega_0) + \Delta\omega_{if}\partial\varphi'(\omega,\omega_0)/\partial\omega_0. \quad (7)$$

Transformation (7) decomposes (4) into the paramagnetic and diamagnetic terms, respectively, which are different in the dispersion shape. However, the paramagnetic term is not yet decomposed into the C term and temperature-independent B term.

At $T \to \infty$, it is obvious that $f_i(T) \to 1/n$, where n is the number of components of the ground state splitting, and one can write the identity

$$f_i(T) \equiv \frac{1}{n} + \left[f_i(T) - \frac{1}{n}\right]. \quad (8)$$

To be more exact, the condition $T \to \infty$ should be replaced by $\Delta E_I \ll kT \ll E_{IK}$, where ΔE_I is the total splitting of the ground multiplet and E_{IK} is the distance to the nearest excited state. If the second of these inequalities is not fulfilled, the sense of the ground state changes. The second component in (8) tends to zero as $1/T$ at $T \to \infty$, the same as the temperature-dependent paramagnetic effect does; therefore, transformation (8) will bring about decomposition of the paramagnetic effect into the B and C terms, respectively, after substituting (7) and (8) into (4):

$$\Delta\alpha_1' = \frac{1}{\hbar}\cdot\frac{\partial\varphi'(\omega,\omega_0)}{\partial\omega_0}\sum_{i,f} f_i(T)\Delta p_{if}^{\pm}\Delta\omega_{if} + \frac{1}{\hbar}\varphi'(\omega,\omega_0) \times\left\{\frac{1}{n}\sum_{i,f}\Delta p_{if}^{\pm} + \sum_{i,f}\left[f_i(T) - \frac{1}{n}\right]\Delta p_{if}^{\pm}\right\}. \quad (9)$$

TABLE I. Experimental paramagnetic MOA (C) at room temperature. Dy2: $Dy_2O_3 + (P_2O_5 - SiO_2 - GeO_2)$, $Dy_2O_3 - 42.3$ mass%. Dy3: $Dy_2O_3 + (La_2O_3 - Al_2O_3 - B_2O_3 - SiO_2 - GeO_2)$, $Dy_2O_3 - 61.8$ mass%. Dy5: $Dy_2O_3 + (La_2O_3 - Al_2O_3 - B_2O_3 - SiO_2 - GeO_2)$, $Dy_2O_3 - 2.65$ mass%.

Transition $^6H_{15/2}(4f^9)\downarrow$	$DyFe_3(BO_3)_4$ This work	Dy2 According to Ref. 22	Dy3 According to Ref. 22	Dy5 According to Ref. 22
$^6(F_{9/2}+H_{7/2})$	−2.3	−0.94	−3.9	−3.2
$^6F_{7/2}$	−4.8	−2.9	−2.9	−4.8
$^6F_{5/2}$	−6.0	−7.5	−5.1	−7.4
$^6F_{3/2}$	−3.5	−6	−6	−7.7

The components in (9) are the most general and rigorous expressions for A, B, and C terms, respectively. In expression (9), the same as in the initial expression (4), the possibility of not completely circular polarization of transitions $i \rightarrow f$ is taken into account, which means a nonzero value of both of the components in (5).

The expression similar to (9) can be considered also in the resonance region and for the MCD, in particular. Then, the condition $\Delta\omega_{if} \ll \gamma_{if}$ should be added, where $\Delta\omega_{if}$ is now the magnetic field splitting of the CF-split components of the transition $I \rightarrow F$. The dispersion functions $\varphi(\omega,\omega_{if},\gamma_{if})$ will now stay under signs of the summations in (9). Integrated over the band $I \rightarrow F$, MCD will contain only paramagnetic terms:

$$\langle \Delta\alpha_1'' \rangle_0 = \frac{1}{\hbar}\left\{ \frac{1}{n}\sum_{i,f} \Delta p_{if}^{\pm} + \sum_{i,f}\left[f_i(T) - \frac{1}{n}\right]\Delta p_{if}^{\pm}\right\}. \quad (10)$$

For the beginning, we shall consider the mixing effect in a free atom for an allowed transition between states with the total moments J_I and J_F. In this case, summation over i and f is replaced by summation over M_I and M_F. According to the Wigner-Eckart theorem, the matrix elements of the spherical components $m = \mp 1$ of the electric dipole moment $\vec{d} = e\vec{r}$, corresponding to the $(\pm)$ circular polarizations of light, are described by the equation

$$\langle k_F J_F M_F | d^{\pm} | k_I J_I M_I \rangle = ei(-1)^{J_{\max}-M_F} \begin{pmatrix} J_F & 1 & J_I \\ -M_F & \mp 1 & M_I \end{pmatrix} \langle k_F J_F || r || k_I J_I \rangle . \quad (11)$$

Here, $\langle k_F J_F || r || k_I J_I \rangle$ is the reduced matrix element, and k_I and k_F are the other quantum numbers. From (11), owing to the properties of the $3j$ symbols, the probabilities of the transitions $M_I \rightarrow M_F$ and $-M_I \rightarrow -M_F$ with opposite circular polarizations are identical. Then, according to (5), (9), and (10), the B term in the birefringence and the integrated over the band $I \rightarrow F$ MCD is equal to zero. However, we had not yet taken into account possible mixing of the states by the spin-orbit interaction and by magnetic field.

The selection rules for the operator $\hat{V}_{SL} = \lambda \hat{S}\hat{L}$ of the spin-orbit interaction have the form

$$\Delta S = 0, \pm 1; \quad \Delta L = 0, \pm 1; \ \Delta J = 0, \ \Delta M = 0. \quad (12)$$

Thus, the operator of the S-L interaction is nondiagonal over S and L but is diagonal over J and M, and its matrix does not depend on M. Operator $\hat{V}_H = \mu_B H (L_z + 2S_z)$ of interaction with the magnetic field is proportional to the z projection of the usual vector, whose decomposition to the spherical-vector projections contains only projection $m = 0$. Then from (11), substituting 0 instead of ∓ 1, one finds that operator $\hat{V}_H$ is nondiagonal over J but is diagonal over M and additionally is diagonal over S, L, M_S, M_L. Because of the properties of the $3j$ symbols, the absolute value of its matrix elements does not depend on the sign of M. Therefore, the account of the mixing of the free atom states by the S-L interaction and by the magnetic field does not violate the symmetry of the transitions $M_I \rightarrow M_F$ and $-M_I \rightarrow -M_F$, and hence the B term is equal to zero in this case as well.

The effect of a CF consists first in the fact that the states with no magnetic moment can arise, which, hence, are not split by the magnetic field. This results in quenching of the diamagnetic and paramagnetic C terms. Meanwhile, such states can demonstrate the effect of the B type, since the magnetic field can bring about circular polarization of transitions with those states taking part. This situation refers to states with the integer total moment.

Any wave function Ψ_i of an atom in an external field can be expressed by a system of orthonormalized wave functions of the free atom Ψ_n:

$$\Psi_i = \sum_n C_{in}\Psi_n, \quad (13)$$

where n are the quantum numbers specifying the chosen system of the free atom functions, and C_{in} is the quadratic matrix. The system of Ψ_n functions may be presented by the wave functions of the J multiplet, by the wave functions of a term, and even by several terms, depending on the approximation chosen to describe the function Ψ_i. The matrix C_{in} performs a unitary transformation and therefore satisfies the relation:

$$\sum_i C_{in}^* C_{in} = 1. \quad (14)$$

This relation means that the pure quantum probability (with the equal population of all states Ψ_i) to find an atom in the state Ψ_n after the external fields are imposed equals that in the free atom. Hence, it follows that at $T \rightarrow \infty$, the B term is always equal to zero if all the functions Ψ_i and Ψ_n, taking part in the transformation (13) caused by external fields applied to the atom, are taken into account in the transition. The B term can differ from zero only in some temperature range from $T = 0$ to $T_{\max}$, when not all states taking part in the transformation (13) are equally thermally populated and, therefore, are not equally taken into account in the transition. Correspondingly, there are two types of the integrated B terms for the $J_I \rightarrow J_F$ transition: 1) due to the mixing of the ground state CF split components not completely populated in the definite temperature range and 2) due to the mixing of the J multiplets. It is possible to show[48] that value of the B term in the former case is

$$b \sim \mu_B H/\Delta, \quad (15)$$

and, in the latter case,

$$b \sim \mu_B H \Delta / E_{SL}^2, \quad (16)$$

where Δ is the CF splitting of the J multiplet and E_{SL} is the spin-orbit splitting, i.e., the distance between mixing J multiplets. In the case of (16) (mixing of the J multiplets), taking into account that $c \sim \mu_B H/kT$, the ratio $b/c \sim kT\Delta/E_{SL}^2$. For R ions, $\Delta \ll E_{SL}$ usually, and at room temperature, $kT \leqslant \Delta$. However, if CF quenches the C term, the B term can be commensurable with the C term at room temperature and can influence the temperature dependence of the total paramagnetic effect. The CF-splitting components of states with the half-integer moment are at least doubly degenerated in any CF and have magnetic moments. Therefore, the C term is not quenched by the CF. Thus, the B term of the type (16) is small compared with the C term in our case.

In the case of (15), the ratio $b/c \sim kT/\Delta$. In the crystal Dy:$YAl_3(BO_3)_4$, isostructural with the studied one, the total CF splitting of the ground state is about 670 K.[6,7] Therefore, even at room temperature, the B term is smaller than the C term, but it can affect the temperature dependence of the total MCD. However, it is evident that existence of the B term cannot bring about the change of sign of the total MCD, which is in contrast to the observation (Fig. 7 and Ref. 22). From Eq. (15), one can think that $b \to \infty$ at $\Delta \to 0$. However, at $\Delta \to 0$, the temperature range of the B-term existence also tends to zero. [The result (Eq. (15)) was illustrated by strict calculations for the transition $3d^1 \to 4p^1$ in Ref. 47.]

It should be noted that measured values k and Δk are not precisely proportional to values α_1'' and $\Delta\alpha_1''$, respectively, which refer to single atoms. It is known that

$$I = I_0 \exp[-k_e x] = I_0 \exp\left[-\frac{2\omega}{c} n'' x\right], \tag{17}$$

where I_0 and I are the incident and transmitted light flows, respectively; k_e is the natural absorption coefficient; n'' is the imaginary part of the complex refraction index; ω is the angular frequency of light; and c is the light speed. From (17),

$$k_e = \frac{2\omega}{c} n'', \tag{18}$$

For the electric dipole transition $n = \sqrt{\varepsilon}$ and according to definition,

$$\varepsilon = 1 + 4\pi\alpha, \tag{19}$$

where α is the polarizability of a unit volume. Then from (18) and (19), one can find that

$$\alpha'' = \frac{cn'}{4\pi\omega} k_e. \tag{20}$$

The electric-dipole moment of the unit volume is

$$P = \alpha E = N\alpha_1 E_{\text{eff}} = N\alpha_1(E + L_1 P) = N\alpha_1 E(1 + L_1\alpha). \tag{21}$$

Here, α_1 is the polarizability of one atom, N is the number of the active atoms in the unit volume, $E_{\text{eff}} = E + L_1 P$ is the effective electric field on the atom, and L_1 is the Lorentz factor. Let us express α via ε from (19) and substitute it only in the right side of (21):

$$\alpha = \alpha_1 N[1 + L_1(\varepsilon - 1)/4\pi] \equiv LN\alpha_1, \tag{22}$$

where L is the Lorentz correction. If the environment of the active atom is close to the spherical one, then $L_1 = 4\pi/3$ and $L = (\varepsilon + 2)/3$. If an electron transition is not a strong one, as in the case of *f-f* transitions, then in the region of this transition $\varepsilon'' \ll \varepsilon'$, and, correspondingly, ε' in this region is conditioned mainly by strong transitions out of the region. Then it is possible to put in (22) $\varepsilon \approx \varepsilon'$ and to refer values α and α_1 only to the *f-f* transition. Then from (20) and (22):

$$\alpha_1'' = \frac{cn'}{4\pi NL\omega} k_e. \tag{23}$$

If one supposes that only k_e changes in the region of the considered *f-f* absorption band, then in this approximation integral paramagnetic MOA is

$$c = \frac{\langle \Delta k(\omega)\rangle_0}{\langle k(\omega)\rangle_0} = \frac{\langle \Delta\alpha_1''(\omega)\rangle_0}{\langle \alpha_1''(\omega)\rangle_0}, \tag{24}$$

and this is true both for natural and decimal coefficient of absorption.

C. Theoretical value of paramagnetic MOA of *f-f* transitions and its comparison with the experimental

f-f transitions become allowed due to admixture of states with opposite parity to $4f$ states by static or dynamic odd components of the CF. Let us consider an admixture of the high energy states with the opposite parity only to an excited $4f$ state, since the former ones are closer to it. In this case, the transition will be allowed if the total angular-momentum selection rule is satisfied for the admixed J_F' state:

$$|J_F' - J_I| \leqslant 1, \tag{25}$$

where J_I is the ground-state total angular momentum. In particular, the f-f transitions from the $J = 15/2$ ground state of the Dy^{3+} ion are allowed due to an admixture of states with $J = 13/2$, $15/2$, and $17/2$ to excited states. All necessary excited states actually exist in a Dy^{3+} ion. Electron states of a Dy^{3+} ion with the $4f^9$ configuration are odd. Consequently, admixed states should be even. These are states with the configuration $4f^8 5d$. The Judd-Ofelt theory for the parity-forbidden *f-f* transitions, allowed by odd components of the CF, gives the selection rule[49]

$$|J_F - J_I| \leqslant \lambda. \tag{26}$$

Here $\lambda = 2$, 4, and 6 for the $4f$ shell. According to Eqs. (25) and (26), the admixed states should satisfy the condition

$$|J_F - J_F'| \leqslant \lambda - 1. \tag{27}$$

All the considered excited states satisfy this condition at least at one value of the parameter λ. Allowed transitions from the ground state to the admixed states provide MOA of the *f-f* transition as well. Thus, the problem of MCD of forbidden *f-f* transitions in condensed matter has reduced to the problem of MCD of allowed transitions in a free atom, and it is necessary to find this MCD.

Let us consider a pair of $\pm M$ states of the ground multiplet of a free atom, which are split in a magnetic field according to the magnetic quantum number $\pm M$. It is known that for an allowed transition in a free atom the integral paramagnetic MOA of transitions from this pair is

$$C_M = g|M|p_M, \tag{28}$$

where C_M is a dimensionless parameter of MOA in units of $\mu_B H/kT$, g is the Landé factor of the ground state, and p_M is the degree of circular polarization of transitions from the $\langle -|M|\rangle$ state, taking into account the polarization sign. Then, the integral MOA of the $J_I \to J_F$ transition is given by

$$C = \sum_{|M|} C_M V_M = g \sum_{|M|} |M| p_M V_M, \tag{29}$$

where V_M is the weight of the pair intensity in the total transition intensity. According to the Wigner-Eckart theorem,

the Zeeman component intensities are proportional to the squared $3j$ symbols:

$$V_M \sim \begin{pmatrix} J_F & 1 & J_I \\ -M_F & \mp 1 & M \end{pmatrix}^2. \tag{30}$$

These quantities are given, e.g., in Ref. 50. From (28) and with the help of Ref. 50, we obtain for the transition $J \to J$:

$$C_M = \frac{-gM^2}{J^2 + J - M^2}, \tag{31}$$

for the transition $J \to (J-1)$:

$$C_M = \frac{-gM^2(2J-1)}{J^2 - J + M^2}, \tag{32}$$

and for the transition $J \to (J+1)$:

$$C_M = \frac{gM^2(2J+3)}{J^2 + 3J + 2 + M^2}. \tag{33}$$

After some transformations from (29)–(33), we find that

$$\begin{aligned} &\text{for the transition } J \to J : C = -g/2, \\ &\text{for the transition } J \to (J-1) : C = -g(J+1)/2, \\ &\text{for the transition } J \to (J+1) : C = +g\ J/2. \end{aligned} \tag{34}$$

These relations are valid for both integer and half-integer angular momenta. It is seen that the paramagnetic MOA is strongly dependent on the excited state. Thus, taking into account that for the ground state $^6H_{15/2}$ the Landé factor $g = 4/3$, one can find possible MOA activities, C, of f-f transitions in a Dy^{3+} ion: -5.66, -0.66, and 5, corresponding to admixtures of states $J = 13/2$, $15/2$, and $17/2$, respectively. First, from Table I, it is seen that maximum observed MOA of f-f transitions are of the same order of magnitude as the theoretical ones. Comparing these values with the experimental data of Table I, it is possible to infer which admixture prevails or several contributions occur into the allowance and MCD of the specific f-f transition. Possibility of variants can result in different MOA of the same f-f transition in different compounds (Table I) that testifies, in turn, to different odd distortions of the local environment of the R ion. In particular, even different concentration of dysprosium in the glasses of the same composition results in a change of the local environment (compare Dy3 and Dy5 glasses in Table I).

Equations (34) are strictly applied to f-f transitions if all sublevels of the CF splitting of the ground state are equally populated. Otherwise, the ratio of the contributions into the MOA can change with the temperature change. This results in a deviation of the MOA temperature dependence from the Curie-Weiss law if several contributions occur. Indeed, the strongest deviation occurs at the transition $\to {}^6(F_{9/2} + H_{7/2})$ in the $DyFe_3(BO_3)_4$ crystal (Fig. 6) and in the Dy2 glass.[22] In these cases, the MOA is the smallest one (Table I), testifying to several contributions to the MOA and to the f-f transition allowance.

All admixtures necessary for allowance of f-f transitions in a Dy^{3+} ion yield to Eq. (27) for the considered excited states. Comparing the experimental (Table I) and the theoretical MOA of the transitions, we conclude that transition $\to {}^6F_{5/2}$ both in $DyFe_3(BO_3)_4$ and in the glasses and transition $\to {}^6F_{3/2}$ in the glasses are allowed only by admixture of the state $J = 13/2$ to the excited states. From Eq. (27), it follows that for the transition $\to {}^6F_{3/2}$ it is the only admixture that allows the transition. MOA of this transition in the $DyFe_3(BO_3)_4$ is smaller as compared with the theoretical one because in the described theory we did not take into account admixtures to the ground state. Corresponding analysis shows that in this case the MOA of the transition $\to {}^6F_{3/2}$ can indeed be smaller.

From Table I, it is seen that some transitions have MOA larger than the theoretical one, according to Eq. (34). How it is possible? CF splitting of the Dy^{3+} ion states in glasses is not known, but it is known in the crystal $Dy{:}YAl_3(BO_3)_4$, isostructural with the studied one.[6,7] The total CF splitting of the ground state is about 670 K. This means that even at room temperature only a part of these states is populated, but the MOA of the populated states differs from the integral MOA. In a first approximation, electronic states in the trigonal electric field are split according to absolute values of M, the same that takes place in the homogeneous electric field. The $DyFe_3(BO_3)_4$ crystal has rather strong magnetic axial anisotropy.[34] Therefore, such approximation can be suitable, and the ground state can have $M = \pm 15/2$. (A real situation will be seen in detail below). The MOA of the transition from the level of such a kind is described by Eqs. (31)–(33). For the mentioned ground state $M = J$, we find

$$\begin{aligned} &\text{for the transition } J \to J : C_M = -gJ, \\ &\text{for the transition } J \to (J-1) : C_M = -gJ, \\ &\text{for the transition } J \to (J+1) : C_M = +gJ. \end{aligned} \tag{35}$$

Comparing Eqs. (35) and (34), one can see that the MOA of the $J_I \to J_F$ absorption band can redouble.

IV. FINE STRUCTURE OF ABSORPTION AND MCD SPECTRA AND PROPERTIES OF 4f STATES

Polarized absorption spectra of all studied f-f transitions are shown in Figs. 8–11. Transition $^6H_{15/2} \to {}^6H_{5/2}$ (Fig. 2) is too

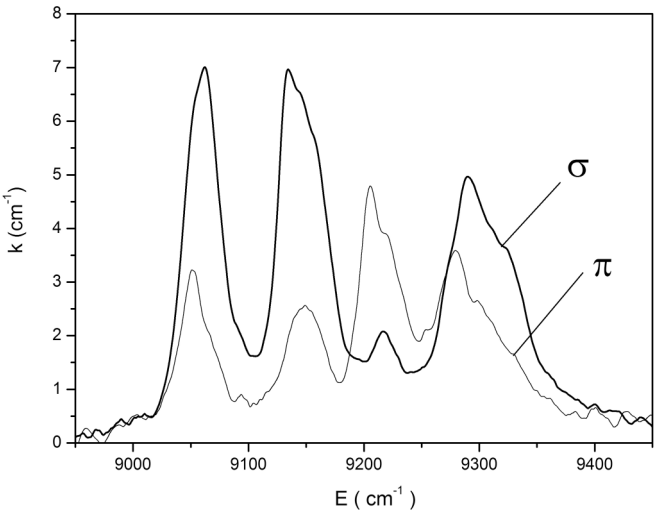

FIG. 8. Polarized absorption spectra of the $^6H_{15/2} \to {}^6(F_{9/2} + H_{7/2})$ transition (A band) at 90 K.

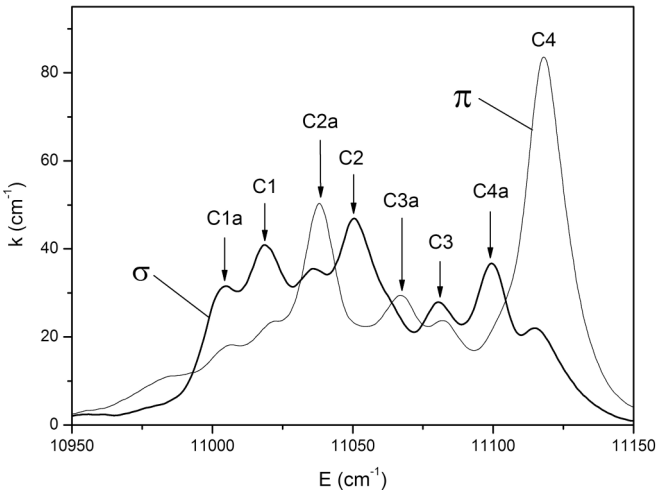

FIG. 9. Polarized absorption spectra of the ${}^6H_{15/2} \rightarrow {}^6F_{7/2}$ transition (C band) at 90 K.

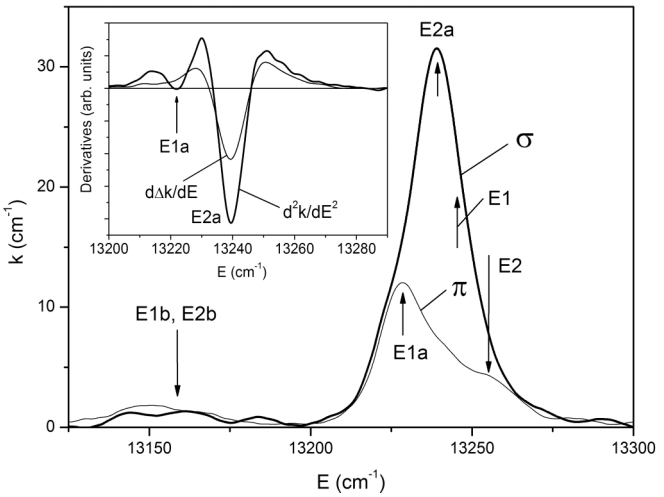

FIG. 11. Polarized absorption spectra of the ${}^6H_{15/2} \rightarrow {}^6F_{3/2}$ transition (E band) at 90 K. Inset: spectra of the first-energy derivative of the MCD spectrum ($d\Delta k/dE$) and of the second-energy derivative of α- (σ-) absorption spectrum (d^2k/dE^2).

weak to be studied. As mentioned above, at $T < 280$ K, the local symmetry of the Dy^{3+} ion is C_2, while symmetry of the whole crystal remains trigonal. In the Dy^{3+} ion with the half-integer total moment degeneracy of states (except the Kramers one) are totally lifted both in C_2 and D_3 symmetries. The only difference between these two symmetries consists of different selection rules for electron transitions. There are two reasons for the analysis of the results in D_3 symmetry approximation. (1) In C_2 symmetry, all transitions are allowed in both polarizations, but our experimental results have shown that it is not so (Figs. 8–11). (2) There are grounds to suppose that deviation of the local symmetry from the D_3 is small. Indeed, at a similar decrease of symmetry from D_3 to C_2 in a $TbFe_3(BO_3)_4$ crystal, a splitting of some states of the Tb^{3+} ion with integer total moment should occur. However, such splitting was not observed.[51] Therefore, we decided that it is quite reasonable to analyze the spectra obtained in a first approximation within the framework of D_3 local symmetry.

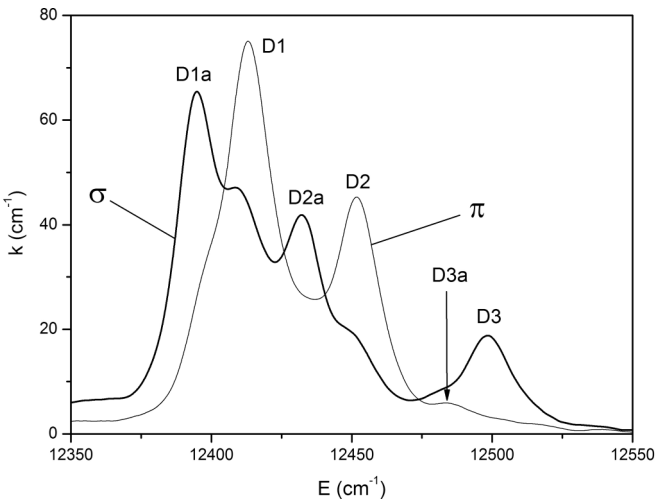

FIG. 10. Polarized absorption spectra of the ${}^6H_{15/2} \rightarrow {}^6F_{5/2}$ transition (D band) at 90 K.

To begin, consider transition ${}^6H_{15/2} \rightarrow {}^6F_{5/2}$ (D) (Fig. 10). The excited state is split in a D_3 trigonal field into three Kramers doublets: ${}^6F_{5/2} \rightarrow 2E_{1/2} + E_{3/2}$. Therefore, one can expect three lines of commensurable value in the spectrum. However, six intensive and closely positioned lines are observed (Fig. 10). Thus, it is possible to suppose that in the ground multiplet there are two close lowest states. Distance between these states (17.4 cm^{-1}) was determined as the average distance between D and Da lines. In the $Dy:YAl_3(BO_3)_4$ crystal, the presence of these close states was theoretically predicted by Cavalli *et al.*[6] at a distance of $\approx$8 cm^{-1} and experimentally determined by Baraldi *et al.*[7] at a distance of 3.3 cm^{-1}. Properties of these states should be identified.

If a crystal has an axis of symmetry, the crystal quantum number μ appears. It is an analog of the magnetic quantum number M of a free atom. In the case of a C_3 axis and a half-integer total moment, there are three possible values of the crystal quantum number[52]: $\mu = +1/2, -1/2$, and $3/2$ ($\pm 3/2$). States with $M = \mu \pm 3n$ (where $n = 0, 1, 2, \ldots$) correspond to each μ in the trigonal symmetry.[52] As a result, the following set of states is obtained:

$$\begin{aligned} M &= \pm 1/2, \pm 3/2, \pm 5/2, \pm 7/2, \pm 9/2, \pm 11/2, \\ &\quad \pm 13/2, \pm 15/2 \\ \mu &= \pm 1/2, (\pm 3/2), \mp 1/2, \pm 1/2, (\pm 3/2), \\ &\quad \mp 1/2, \pm 1/2, (\pm 3/2) \end{aligned} \tag{36}$$

The set of the CF states for J multiplets of the Dy^{3+} ion is found according to the value of J. States with $\mu = \pm 1/2$ correspond to states $E_{1/2}$, and states with $\mu = (\pm 3/2)$ correspond to states $E_{3/2}$ in the D_3 group notations. In crystals, selection rules for the polarized light absorption are governed by the number μ, and they coincide with those for the number M in a free atom.[52]

In particular, for the electric dipole absorption,

$$\Delta\mu = \pm 1 \text{ corresponds to } \mp \text{circularly polarized and } \sigma\text{-polarized waves},$$
$$\Delta\mu = 0 \text{ corresponds to } \pi\text{-polarized waves.} \tag{37}$$

For linearly polarized waves, these selection rules coincide naturally with that of Table II.

In a homogeneous electric field ($C_{\infty v}$ symmetry), atomic states are split according to the absolute value magnetic quantum number M. In a first approximation, electron states in the trigonal electric field are also split according to absolute values of M. As mentioned above, the $DyFe_3(BO_3)_4$ crystal has rather strong axial magnetic anisotropy.[34] Therefore, such first approximation is possible, and Dy wave functions can be described by $|J,\pm M_J\rangle$ states. Thus, there are two candidates for the lowest states: $E_{1/2}$ ($M = \pm 13/2$) and $E_{3/2}$ ($M = \pm 15/2$). In the former case, according to selection rules of Table II, there should be transitions 2π, $\sigma + \sigma$ and, in the latter case, $2\sigma + \pi$. Polarizations of not all lines are reliably seen directly from absorption spectra (Fig. 10), but they can be found from the second derivatives of the absorption spectra (Figs. 12 and 13). Negative extrema of the second derivative correspond to the absorption lines. Experimentally observed linear polarizations of transitions from the lowest level (Fig. 14) show that it is state $E_{1/2}$ ($M = \pm 13/2$). The $D3a$ line has comparable σ and π polarizations (Figs. 10, 12, and 13), that differs from the theoretically predicted pure π polarization (shown in bracket in Fig. 14). $D1a$ and $D2a$ lines have mainly σ polarizations (bold symbols in Fig. 14), which correspond to the theoretical prediction. A neutron diffraction study of $DyFe_3(BO_3)_4$ at 1.5 K (1.04 cm^{-1}),[39] when only the lowest level is occupied, gave 6.4 μ_B for the Dy magnetic moment that is close to 6.5 μ_B of the above identified lowest state $E_{1/2}$ ($M = \pm 13/2$).

Fine structure of the MCD spectra (Figs. 3–6) is evidently due to the diamagnetic effect. The Zeeman splitting of an absorption line $2\Delta\omega_0$ is found through the Zeeman splitting of the initial and final levels,

$$2\hbar\Delta\omega_0 = \pm(\Delta E_i \pm \Delta E_f). \tag{38}$$

The splitting of the Kramers doublets in a magnetic field directed along the C_3 axis of a crystal is represented in the form:

$$\Delta E = \mu_B g_C H, \tag{39}$$

where g_C is the effective Landé factor in the C_3 direction. Therefore, for the Kramers doublets,

$$2\hbar\Delta\omega_0 = \mu_B H \Delta g_C. \tag{40}$$

TABLE II. Selection rules for electric-dipole transitions in D_3 symmetry.

	$E_{1/2}$	$E_{3/2}$
$E_{1/2}$	$\pi, \sigma(\alpha)$	$\sigma(\alpha)$
$E_{3/2}$	$\sigma(\alpha)$	π

Sign of the temperature-dependent paramagnetic effect [c in Eq. (2)] is defined by polarization of the transition from the lower component of the Zeeman splitting of the initial state. The sign of the diamagnetic effect [$\Delta\omega_0$ in Eq. (2)] is not so unambiguous. The first sign in (38) refers to the sign of the paramagnetic effect, and the second one shows that the splitting of states can sum up and subtract (see below).

Let us assume that absorption lines in (1) have the Gaussian shape:

$$\varphi_\pm = \exp[-(\omega - \omega_0 \pm \Delta\omega_0)^2/2\sigma^2], \tag{41}$$

where σ characterizes the width of the absorption line (it is the half width at the level $\sqrt{e} = 0.606$ of the maximum). From (41) it is evident that $\partial\varphi(\omega,\omega_0)/\partial\omega = -\partial\varphi(\omega,\omega_0)/\partial\omega_0$. Then, according to Eq. (2), if signs of $\partial k/\partial\omega$ and $\Delta k(\omega)$ coincide, the diamagnetic effect $\Delta\omega_0$ is negative and vise versa. However, it is more convenient to compare $\partial^2 k/\partial\omega^2$ and $\partial\Delta k/\partial\omega$. Positions of negative extrema of the former function give positions of absorption lines. Signs of extrema of the latter function at these positions give signs of the diamagnetic effect (see Fig. 12). Thus, diamagnetic effects of all transitions in the D band, except $D3a$, are negative (this is marked in Fig. 14). In the same approximation, as Eq. (2) was obtained ($\Delta\omega_0 \ll \sigma$), it is possible to find that

$$\Delta\omega_0 = \langle\Delta k(\omega)\rangle_1/\langle k(\omega)\rangle_0. \tag{42}$$

The first moment is calculated relative to ω_0 and is equal to zero for the paramagnetic effect. Equation (42) is valid only for one solitary pair of the Zeeman-splitting components.

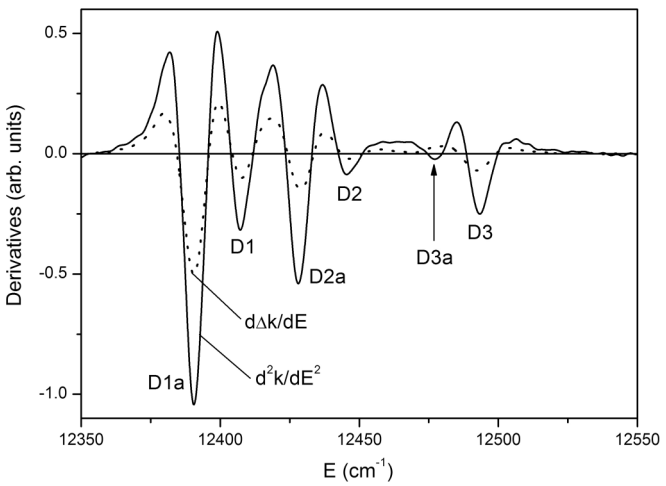

FIG. 12. Spectra of the first-energy derivative of the MCD spectrum ($d\Delta k/dE$) and of the second-energy derivative of α- (σ-) absorption spectrum (d^2k/dE^2) of ${}^6H_{15/2} \rightarrow {}^6F_{5/2}$ transition (D band) at 90 K.

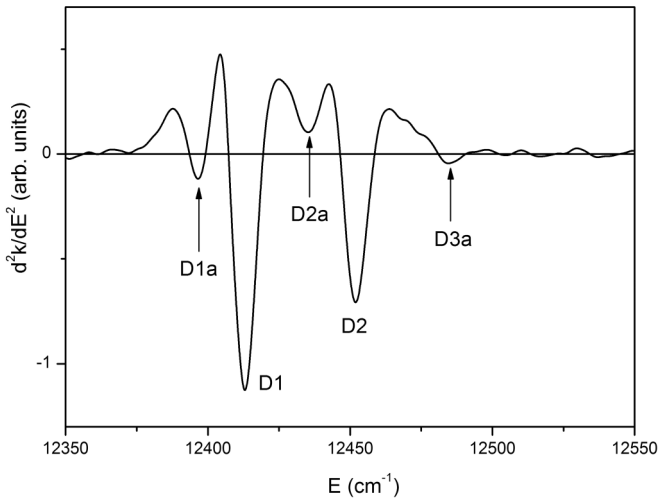

FIG. 13. Spectrum of the second-energy derivative of the π-absorption spectrum (d^2k/dE^2) of the ${}^6H_{15/2} \rightarrow {}^6F_{5/2}$ transition (D band) at 90 K.

It is more convenient to find the Zeeman splitting with the help of values (Δk_{dm}) and positions (ω_m) of extrema of the diamagnetic effect and amplitude (k_m) of the α (σ) absorption line. For the Gaussian $|\omega_m - \omega_0| \approx \sigma$ and

$$\Delta\omega_0 = \frac{\Delta k_{dm}}{k_m} |\omega_m - \omega_0| \sqrt{e}. \tag{43}$$

In the case of the Lorentzian form function, $\sqrt{e}$ should be replaced by 2. If the paramagnetic effect $c \ll 1$, then the mentioned parameters of the diamagnetic spectrum coincide with those of the total MCD spectrum of the absorption line. Thus, from the parameters of α absorption and MCD spectra, one can find the Zeeman splitting of the absorption lines and corresponding differences of the effective Landé factors Δg_C of states according to (40).

In particular, in the D band it is possible to estimate the Zeeman splitting of $D1a$ and $D3$ lines. For the $D1a$ line (Figs. 5 and 10), it was obtained $2\Delta\omega_0 = -0.866$ cm^{-1} kOe^{-1} and $\Delta g_C = -18.5$. For the $D3$ line, it was obtained $2\Delta\omega_0 = -0.619$ cm^{-1} kOe^{-1} and $\Delta g_C = -13.2$. Values of Δk_{dm}

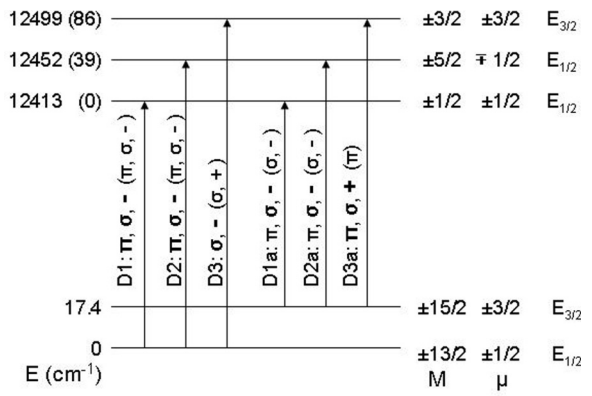

FIG. 14. Diagram of f-f transitions and the crystal-field levels of ${}^6H_{15/2} \rightarrow {}^6F_{5/2}$ (D) absorption band. Prevailing experimental observed polarizations are shown in bold. The theoretically expected polarizations are shown in parentheses.

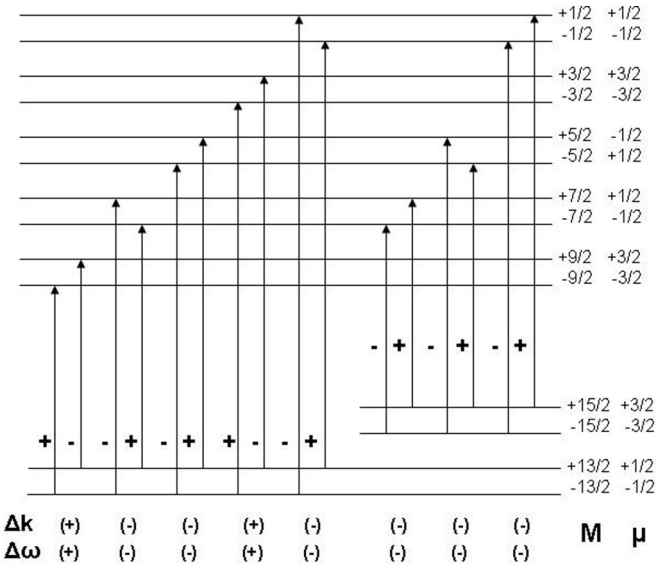

FIG. 15. General schematic diagram of f-f transitions in a Dy^{3+} ion and their circular polarizations in magnetic field directed along the C_3 axis.

were found as the half sum of positive and negative extrema, and value k_m was found as a result of decomposition of the α-absorption spectrum into the Lorentz curves.

If an atom is in a magnetic field directed along the homogeneous electric field, each of states with the quantum number $\pm M$ is split. The value of the splitting is

$$\Delta E = 2g\mu_B MH \tag{44}$$

under the following condition: that this splitting is much less than the splitting in the electric field. Here g is the Landé factor of the free atom. Equation (44) can also be applied in the case of the axially symmetric CF with M_{eff} instead of M, since states [Eq. (36)] can contain admixtures of states with different M that belong to the same number μ. This is so because the matrix of the CF on the basis of the free atom functions is not diagonal over M in the trigonal symmetry. According to (44) and (39), one can find maximum possible values of splitting of the Kramers doublets in magnetic field along C_3 axis and maximum possible values of g_C

$$g_{C\,\max} = 2gM \tag{45}$$

for all doublets of the ground and excited multiplets of Dy^{3+} ion (Table III).

With the help of (36) and (37), taking into account in a first approximation splitting [Eq. (44)] in a magnetic field according to $\pm M$ and splitting in the CF according to $|M|$, the general schematic diagram of transitions and their polarizations in the magnetic field directed along the C_3 axis can be created (see Fig. 15). When the splitting of a line is equal to the difference of the splitting of the states [minus sign in (38) in brackets] and these splittings are close in value, the sign of the line splitting is in question.

Now, with the help of Fig. 15, the theoretically expected circular polarizations of transitions in the D band can be found (see Fig. 14). For lines $D1$, $D2$, $D1a$, and $D2a$, the theoretical predictions coincide with the experimental. For the $D3$ line, the expected sign is opposite to the observed one, and for the $D3a$

TABLE III. Maximum possible effective Landé factors of states along the C_3 axis of a crystal.

	M	15/2	13/2	9/2	7/2	5/2	3/2	1/2
$^6H_{15/2}$, $g = 1.333$	$g_{C\max}$	20	17.33	12	9.33	6.66	4	1.33
$^6F_{3/2}$, $g = 1.066$	$g_{C\max}$						3.2	1.066
$^6F_{5/2}$, $g = 1.314$	$g_{C\max}$					6.57	3.94	1.314
$^6F_{7/2}$, $g = 1.397$	$g_{C\max}$				9.78	6.98	4.19	1.397

line, circular polarization was not expected at all. According to (38), Figs. 14, 15, and Table III, the expected maximum Δg_C for the $D1a$ transition is $-(g_i - g_f) = -18.7$, which is close to the experimentally found value -18.5. For the $D3$ transition $\Delta g_{C\max} = +(g_i - g_f) = +13.4$, which is close in absolute value but opposite in sign to the experimentally found $\Delta g_C = -13.2$.

MCD and absorption spectra of the E band ($^6H_{15/2} \rightarrow {}^6F_{3/2}$) and their derivatives are shown in Figs. 6 and 11. These figures give linear and circular polarizations of lines presented in the diagram of Fig. 16. The excited state is split in the trigonal field D_3 into two Kramers doublets: $^6F_{3/2} \rightarrow E_{1/2} + E_{3/2}$. From the lowest state $E_{1/2}$ ($M = \pm 13/2$), there should be transitions π, $\sigma + \sigma$, and from the next state $E_{3/2}$ ($M = \pm 15/2$), $\pi + \sigma$ transitions. The most probable identification of the transitions is depicted in Figs. 11 and 16. $E1b$ and $E2b$ lines (Fig. 11) correspond to transitions from the next state of the ground manifold at energy $\sim$80 cm^{-1}. The theoretical signs of the diamagnetic MCD were found with the help of Fig. 15. Prevailing polarizations of $E1a$ and $E2a$ lines coincide with the theoretical predictions. $E1$ and $E2$ lines are weak and slightly influence the spectra. Distance between the lowest states of the ground multiplet, found from the E spectrum as the distance between lines $E2$ and $E2a$, is 16 cm^{-1}. MCD (Fig. 6) and α-absorption spectra are permitted to find the diamagnetic effect $2\Delta\omega_0 = -1.01$ cm^{-1} kOe^{-1} and corresponding $\Delta g_C = -17.8$ for the $E2a$ transition. According to (38), Figs. 15, 16, and Table III, $\Delta g_{C\max} = -(20 - 1.066) = -18.9$ for this transition, which is close to the experimentally found value.

MCD and absorption spectra of the C band ($^6H_{15/2} \rightarrow {}^6F_{7/2}$) are shown in Figs. 4 and 9, respectively. The excited state is split in the trigonal D_3 field into four Kramers doublets: $^6F_{7/2} \rightarrow 3E_{1/2} + E_{3/2}$. From the lowest state $E_{1/2}$ ($M = \pm 13/2$), there should be transitions 3π, $\sigma + \sigma$, and from the next state $E_{3/2}$ (m $= \pm 15/2$), $3\sigma + \pi$ transitions. Linear polarizations of the absorption lines were found from the second derivatives of the absorption spectra (Figs. 17 and 18). The set of the theoretically expected linear polarizations of transitions from the lowest state ($E_{1/2}$) coincides with the experimental one for prevailing polarizations and gives identification of the excited states of the C band (Fig. 19). The set of the theoretically expected polarizations of transitions from the next state ($E_{3/2}$) does not coincide with the theoretical one (Fig. 19) for any identification of the excited states. Expected linear polarizations of transitions from the $E_{3/2}$ state in the case of the above identification of the excited states are shown in Fig. 19 in parentheses. Signs of the diamagnetic effects are found from the comparison of derivatives of absorption and MCD spectra (Fig. 17), as described above. Expected signs of the diamagnetic effects, found from Fig. 15 assuming the identification of states in Fig. 19, are shown in Fig. 19 in parentheses. The splitting between the lowest sublevels of the ground multiplet found from the C band is 16 cm^{-1}. Thus, the average splitting found from three bands is 16.5 cm^{-1}.

It is practically impossible to interpret absorption (Fig. 8) and MCD (Fig. 3) spectra of the $^6H_{15/2} \rightarrow {}^6(F_{9/2} + H_{7/2})$ transition (A band), since two multiplets are superimposed in energy and the wave functions are heavily mixed. Comparatively weak absorption lines observed from the lower energy

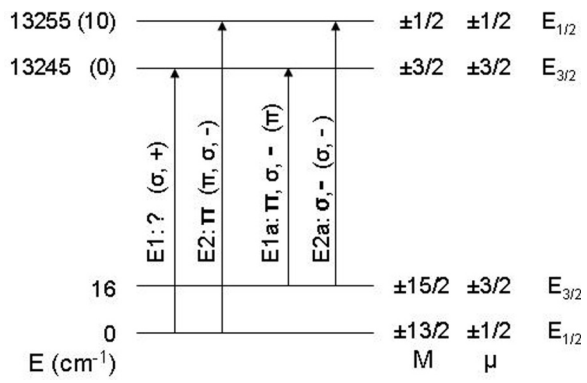

FIG. 16. Diagram of f-f transitions and the crystal-field levels of the $^6H_{15/2} \rightarrow {}^6F_{3/2}$ (E) absorption band. Prevailing experimental observed polarizations are shown in bold. The theoretically expected polarizations are shown in parentheses.

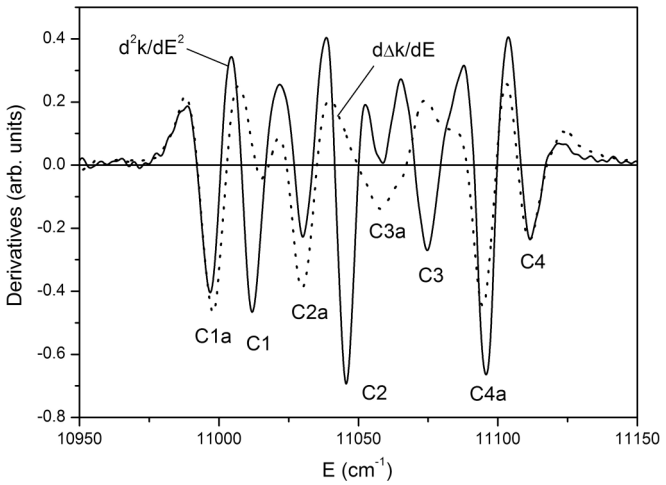

FIG. 17. Spectra of the first-energy derivative of MCD spectrum ($d\Delta k/dE$) and of the second-energy derivative of the α-(σ-) absorption spectrum (d^2k/dE^2) of the $^6H_{15/2} \rightarrow {}^6F_{7/2}$ transition (C band) at 90 K.

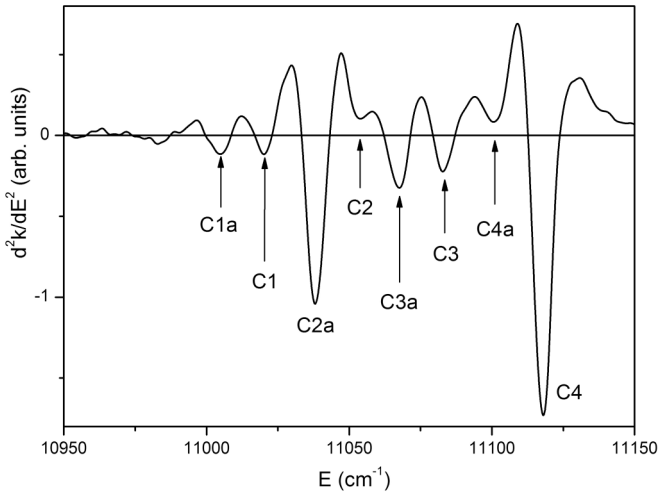

FIG. 18. Spectrum of the second-energy derivative of π-absorption spectrum (d^2k/dE^2) of the ${}^6H_{15/2} \rightarrow {}^6F_{7/2}$ transition (C band) at 90 K.

side of the main bands at 90 K and at higher temperatures (e.g., see Fig. 11) give positions of some higher levels of the ground manifold. Approximate positions of these levels are 80, 105, 175, 215, and 275 cm^{-1}.

Linear polarizations of transitions from the lowest level of the ground state in C and D bands (Figs. 19 and 14) confirm that this lowest state is of $E_{1/2}$ type in D_3 symmetry approximation, and that this symmetry is suitable for description of these transitions. Polarizations of transitions from the second level of the ground manifold obey the assignment $E_{3/2}$ in D_3 symmetry for this state in the E band (Fig. 16), deviate a little from this assignment in the D band (Fig. 14), and strongly deviate in the C band (Fig. 19). In C_2 local symmetry, all transitions are allowed in both linear polarizations. Signs of the Zeeman effect also do not always coincide with the expected ones (Figs. 14, 16, and 19). Circular polarizations are some average macroscopic results of the light interaction with three equivalent centers of C_2 site symmetry. Thus, all observed discrepancies between the experiment and predictions based on the D_3-site symmetry assumption can be supposed to be conditioned by the C_2 distortions. However, these discrepancies take place

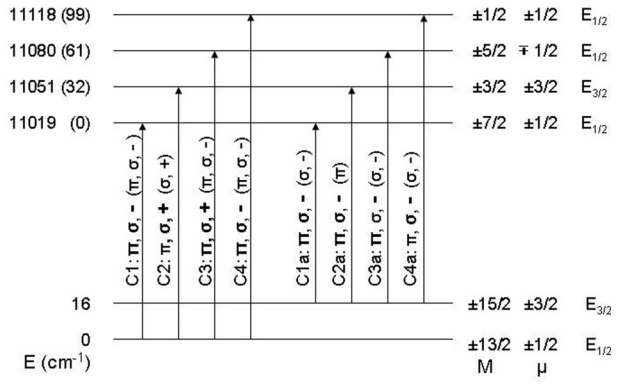

FIG. 19. Diagram of f-f transitions and crystal-field levels of the ${}^6H_{15/2} \rightarrow {}^6F_{7/2}$ (C) absorption band. Prevailing experimental observed polarizations are shown in bold. The theoretically expected polarizations are shown in parentheses.

only at some electron transitions. Consequently, it is possible to infer that in the process of some electron transitions, the local environment of the Dy^{3+} ion changes stronger than it takes place in the ground state, and these changes depend not only on the excited but also on the initial state. Indeed, crystal structure directly depends on the electronic structure of the atoms of the crystal. An electronically excited atom is, actually, an impurity atom, and, consequently, the geometry of its local environment can change. This statement does not necessarily mean that the atom really changes its position during the electron transition, but rather that it is not in an equilibrium position for the excited state since the interaction of the R ion with ligands changes. The change of the position (i.e., deviation from the adiabatic approximation) can also take place, and this can be revealed in luminescence.[53] In addition, an electron transition is not an instant event but a process, which occurs within some period of time. According to the perturbation theory, electron transitions occur due to the mixing of initial and final states by the time-dependent perturbation caused by an electromagnetic wave. Therefore, during the electron transition, the initial state of the ion and its interaction with the environment also changes and can have an influence on the polarization of transitions that was actually observed. Indeed, linear polarizations of transitions from the lowest level of the ground state in C and D bands agree with the D_3 symmetry, but polarizations of transitions to the same states from the next level of the ground state partially disagree with the D_3 symmetry assumption. Spectroscopic manifestations of local distortions connected with electronic transitions were earlier observed also in some other R-containing crystals of huntite structure: $TmAl_3(BO_3)_4$ (see Ref. 54), $YbAl_3(BO_3)_4$ (see Ref. 55), $TbFe_3(BO_3)_4$ (see Ref. 51), and $Nd_{0.5}Gd_{0.5}Fe_3(BO_3)_4$ (see Ref. 40).

V. SUMMARY

MCD and polarized optical absorption spectra of single-crystal $DyFe_3(BO_3)_4$ were measured in the region of the crystal transparency from 8700 to 16 000 cm^{-1} in the temperature range from 90 K up to room temperature. Spectra of d-d and f-f transitions were separated, and f-f transitions ${}^6H_{15/2} \rightarrow {}^6(F_{9/2} + H_{7/2})$, ${}^6F_{7/2}$, ${}^6F_{5/2}$, and ${}^6F_{3/2}$ were studied. From these measurements, temperature dependences of the paramagnetic MOA of the electric dipole forbidden f-f transitions were obtained. It was revealed that, in contrast to allowed transitions, temperature dependences of the MOA of some f-f transitions substantially deviate from the Curie-Weiss law. Comparison with Dy-containing glasses has shown that, also in contrast to allowed transitions, values of MOA of the same f-f transitions strongly depend on the Dy environment. The theory of MOA of allowed and f-f transitions was considered and compared with the experimental results. It was shown that (1) maximum MOA of f-f transitions is the same as that of allowed transitions; (2) the MOA of f-f transitions can consist of several contributions of different values and signs; (3) the ratio of the contributions is determined by the symmetry of the CF; and (4) the ratio of the contributions depends on the population of components of the ground-state CF splitting, which results in deviation of the MOA temperature dependence from the Curie-Weiss law.

Circular polarizations in the magnetic field and linear polarizations of absorption lines were determined. Symmetries of the CF states were analyzed on the basis of the obtained results. A small splitting ($\approx$16.5 cm^{-1}) between the two lowest sublevels of the ground manifold was detected, and symmetries of these states were identified as $E_{1/2}$ ($M = \pm 13/2$) and $E_{3/2}$ ($M = \pm 15/2$), respectively, in the D_3 local symmetry approximation. The Zeeman splitting of some absorption lines and changes of the Landé factor at the corresponding transitions were found. They are close to the maximum possible ones for the axially symmetric crystal. At $T < 280$ K, the local symmetry of Dy^{3+} ion is C_2. However, deviation from D_3 symmetry is small, and it was revealed that the polarizations of the majority of absorption lines can be accounted for in D_3 local symmetry. This also indicates that in the process of some other electron transitions, the equilibrium configuration of the local environment deviates from D_3 symmetry stronger than it does in the ground state. In addition, it has been shown that the distortions depend not only on the excited but also on the initial state since electron transitions occur due to the mixing of initial and final states by the time-dependent perturbation caused by an electromagnetic wave.

ACKNOWLEDGMENTS

The work was supported by the Russian Foundation for Basic Researches Grant No. 12-02-00026 and by the Russian President Grant No. SS-1044.2012.2.

*Corresponding author: malakha@iph.krasn.ru

[1] J. Hormadaly and R. Reisfeld, J. Non-Cryst. Solids **30**, 337 (1979).
[2] Y. Guimond, J. L. Adam, A. M. Yurdyc, J. Mugnier, B. Jacquier, and X. H. Zhang, Opt. Mater. **12**, 467 (1999).
[3] P. Babu and C. K. Jayasankar, Opt. Mater. **15**, 65 (2000).
[4] G. Dominiak-Dzik, P. Solarz, W. Ryba-Romanowski, E. Beregi, and L. Kovács, J. Alloys Compd. **359**, 51 (2003).
[5] J. B. Gruber, B. Zandi, U. V. Valiev, and Sh. A. Rakhimov, J. Appl. Phys. **94**, 1030 (2003).
[6] E. Cavalli, E. Bovero, N. Magnani, M. O. Ramirez, A. Speghini, and M. Bettinelli, J. Phys.: Condens. Matter **15**, 1047 (2003).
[7] A. Baraldi, R. Capelletti, N. Magnani, M. Mazzera, E. Beregi, and I. Földvari, J. Phys.: Condens. Matter. **17**, 6245 (2005).
[8] L. Rama Moorthy, A. Radhapathy, M. Jayasimhadri, D. V. R. Moorthy, and R. V. S. S. N. R. Kumar, J. Alloys Compd. **408–412**, 724 (2006).
[9] F. Yen, B. Lorenz, Y. Y. Sun, C. W. Chu, L. N. Bezmaternykh, and A. N. Vasiliev, Phys. Rev. B **73**, 054435 (2006).
[10] A. M. Kadomtseva, Yu. F. Popov, G. P. Vorob'ev, A. A. Muhin, V. Yu. Ivanov, A. M. Kuzmenko, and L. N. Bezmaternykh, Pisma v ZhETF **87**, 45 (2008) [JETP Lett. **87**, 39 (2008)].
[11] R. P. Chaudhury, F. Yen, B. Lorenz, Y. Y. Sun, L. N. Bezmaternykh, V. L. Temerov, and C. W. Chu, Phys. Rev. B **80**, 104424 (2009).
[12] A. K. Zvezdin, S. S. Krotov, A. M. Kadomtseva, G. P. Vorob'ev, Yu. F. Popov, A. P. Pyatakov, L. N. Bezmaternykh, and E. A. Popova, JETP Lett. **81**, 272 (2005).
[13] A. K. Zvezdin, G. P. Vorob'ev, A. M. Kadomtseva, Yu. F. Popov, A. P. Pyatakov, L. N. Bezmaternykh, A. V. Kuvardin, and E. A. Popova, JETP Lett. **83**, 509 (2006).
[14] N. F. Borelli, J. Chem. Phys. **41**, 3289 (1964).
[15] J. H. Van Vleck and M. H. Hebb, Phys. Rev. **46**, 17 (1934).
[16] S. J. Collocott and K. N. R. Taylor, J. Phys. C **11**, 2885 (1978).
[17] S. J. Collocott and K. N. R. Taylor, J. Phys. C **12**, 1767 (1979).
[18] A. A. Klochkov, U. V. Valiev, and A. S. Moskvin, Phys. Status Solidi B **167**, 337 (1991).
[19] K. Binnemans, C. Gorller-Walrand, J. Lucas, N. Duhamel, and J. L. Adam, J. Alloys Compd. **225**, 80 (1995).
[20] K. Binnemans, D. Verboven, C. Gorller-Walrand, J. Lucas, N. Duhamel-Henry, and J. L. Adam, J. Alloys Compd. **250**, 321 (1997).
[21] A. V. Malakhovskii, V. A. Isachenko, A. L. Sukhachev, A. M. Potseluyko, V. N. Zabluda, T. V. Zarubina, and I. S. Edelman, Fizika Tverdogo Tela **49**, 667 (2007) [Phys. Solid State **49**, 701 (2007)].
[22] A. L. Sukhachev, A.Yu. Strokova, and A. V. Malakhovskii, Solid State Phenomena **168-169**, 557 (2011).
[23] R. W. Schwartz, T. R. Faulkner, and F. S. Richardson, Mol. Phys. **38**, 1767 (1979).
[24] I. V. Ignat'ev and V. V. Ovsyankin, Opt. Spektrosk. **76**, 965 (1994) [Opt. Spectrosc. **76**, 862 (1994)].
[25] L. Fluyt, I. Couwenberg, H. Lambaerts, K. Binnemans, C. Görller-Walrand, and M. F. Reid, J. Chem. Phys. **105**, 6117 (1996).
[26] L. Fluyt, E. Hens, H. De Leebeeck, C. Gorller-Walrand, and K. U. Leuven, J. Alloys Compd. **250**, 316 (1997).
[27] I. Couwenberg and C. Gorller-Walrand, J. Alloys Compd. **275–277**, 388 (1998).
[28] C. Bonardi, R. A. Carvalho, H. C. Basso, M. C. Terrile, G. K. Cruz, L. E. Bausa, and J. Garcia Sole, J. Chem. Phys. **111**, 6042 (1999).
[29] H. De Leebeeck, K. Binnemans, and C. Görller-Walrand, J. Alloys Compd. **291**, 300 (1999).
[30] A. V. Malakhovskii, I. S. Edelman, A. L. Sukhachev, V. V. Markov, and V. N. Voronov, Opt. Mater. **32**, 243 (2009).
[31] A. V. Malakhovskii, U. V. Valiev, I. S. Edelman, A. E. Sokolov, I. Yu. Chesnokov, and I. A. Gudim, Opt. Mater. **32**, 1017 (2010).
[32] A. L. Sukhachev, A. V. Malakhovskii, I. S. Edelman, V. N. Zabluda, V. L. Temerov, and I. Ya. Makievskii, J. Magn. Magn. Mater. **322**, 25 (2010).
[33] Y. K. Zhou, S. Emura, S. Hasegawa, and H. Asahi, Physica Status Solidi C **8**, 2173 (2011).
[34] I. A. Gudim, A. I. Pankrats, E. I. Durnaykin, G. A. Petrakovskiy, L. N. Bezmaternykh, R. Szymczak, and M. Baran, Crystallogr. Rep. **53**, 1140 (2008).
[35] Y. Hinatsu, Y. Doi, K. Ito, K. Wakeshima, and A. Alemi, J. Solid State Chem. **172**, 438 (2003).
[36] E. A. Popova, N. Tristan, A. N. Vasiliev, V. L. Temerov, L. N. Bezmaternykh, N. Leps, B. Büchner, and R. Klingeler, Eur. Phys. J. B **62**, 123 (2008).
[37] S. A. Klimin, D. Fausti, A. Meetsma, L. N. Bezmaternykh, P. H. M. van Loosdrecht, and T. T. M. Palstra, Acta Crystallogr. Sect. B **61**, 481 (2005).

[38]D. Fausti, A. A. Nugroho, P. H. M. van Loosdrecht, S. Klimin, M. N. Popova, and L. N. Bezmaternykh, Phys. Rev. B **74**, 024403 (2006).
[39]C. Ritter, A. Pankrats, I. Gudim, and A. Vorotynov, J. Phys.: Conference Series **340**, 012065 (2012).
[40]A. V. Malakhovskii, S. L. Gnatchenko, I. S. Kachur, V. G. Piryatinskaya, A. L. Sukhachev, and I. A. Gudim, J. Alloys Compd. **542**, 157 (2012).
[41]A. V. Malakhovskii, I. S. Edelman, Y. Radziner, Y. Yeshurun, A. M. Potseluyko, T. V. Zarubina, A. V. Zamkov, and A. I. Zaitzev, J. Magn. Magn. Mater. **263**, 161 (2003).
[42]P. J. Stephens, J. Chem. Phys. **52**, 3489 (1970).
[43]P. J. Stephens, Adv. Chem. Phys. **35**, 197 (1976).
[44]S. B. Piepho and P. N. Schatz, *Group Theory in Spectroscopy: With Applications to Magnetic Circular Dichroism* (John Wiley & Sons, New York, 1983).
[45]C. Görller-Walrand and L. Fluyt, in *Handbook on the Physics and Chemistry of Rare Earths*, edited by K. A. Gschneidner, Jr., J.-C. G. Bünzli, and V. K. Pecharsky, Vol. 40 (B. V. Elsevier, Amesterdam, 2010), pp. 2–107.
[46]R. Serber, Phys. Rev. **41**, 489 (1932).
[47]A. V. Malakhovskii, Phys. Status Solidi **106**, 327 (1981).
[48]A. V. Malakhovskii, Phys. Status Solidi B **159**, 883 (1990).
[49]R. D. Peacock, Structure and Bonding **22**, 83 (1975).
[50]I. I. Sobel'man, *Introduction to the Theory of Atomic Spectra* (Pergamon, Oxford, 1972; Nauka, Moscow, 1977).
[51]A. V. Malakhovskii, S. L. Gnatchenko, I. S. Kachur, V. G. Piryatinskaya, A. L. Sukhachev, and V. L. Temerov, Eur. Phys. J. B **80**, 1 (2011).
[52]M. A. El'yashevitch, *Spectra of rear earths* (GIT-TL, Moskow, 1953, in Russian).
[53]W. W. Holloway, E. W. Prohovsky, and M. Kestigian, Phys. Rev. **139**, A954 (1965).
[54]A. V. Malakhovskii, I. S. Edelman, A. E. Sokolov, V. L. Temerov, S. L. Gnatchenko, I. S. Kachur, and V. G. Piryatinskaya, J. Alloys Compd. **459**, 87 (2008).
[55]A. V. Malakhovskii, A. L. Sukhachev, S. L. Gnatchenko, I. S. Kachur, V. G. Piryatinskaya, V. L. Temerov, A. S. Krylov, and I. S. Edelman, J. Alloys Compd. **476**, 64 (2009).